In-line D-fiber electric field sensor using chiral liquid crystals

S. M. Chandani[*a], N.A.F. Jaeger[a], R-F. Shao[b], J.E. Maclennan[b]

[a]Dept. of Electrical & Computer Engineering, University of British Columbia, Vancouver, BC, Canada
[b]Dept. of Physics and Liquid Crystal Materials Research Center, University of Colorado, Boulder, CO, USA

ABSTRACT

Optical electric field sensors have been used for the measurement of high-voltages found in power substations. Typical sensors are based on electro-optic crystals and hence require the coupling of light into and out of the crystals from optical fibers. This coupling is difficult and costly. The objective of the work presented here is the design and implementation of an optical electric field sensor that uses an entirely fiber-based sensor-head. The sensor-head is comprised of a D-shaped optical fiber with its flat side coated with liquid crystals. D-fibers allow easy access to the evanescent optical field and replacement of part of the cladding with an external medium allows for modulation of this optical field. We are investigating the use of chiral Smectic A liquid crystals, which respond linearly to electric fields through the electroclinic effect. The propagation characteristics of the D-fiber for various distances between the fiber core edge and flat and for various refractive indices of the external medium are theoretically investigated and experimentally verified. Preliminary experimental results for a prototype electric field sensor are presented. The sensor responds in a linear fashion to an applied electric field.

Keywords: electric field sensor, D-fiber, chiral liquid crystal, evanescent field

1. INTRODUCTION

Optical and fiber-optic sensors are increasingly replacing traditional transducers in many applications such as accelerometers, gyroscopes, position sensors and voltage and current sensors. Such sensors have proven to be very accurate, have larger dynamic ranges and bandwidths and, in many cases, are more environmentally friendly than conventional technologies.

Optical electric field sensors are normally used for voltage and current measurement and were first investigated in the 1970's[1,2,3,4]. In most cases, these sensors used electro-optic and/or magneto-optic crystals with free space optical links and components. With the advent of high-quality optical fibers, cost effective fiber-optic components, and integrated-optics, in the past two decades, free space optics and links have been replaced by their fiber-optic and integrated-optic counterparts. However, typically the sensor-heads are still crystal based and, hence, require coupling of light into and out of optical fibers which adds significant cost.

These crystal-based sensors are based on the linear electro-optic (or Pockels) effect, which causes a linear change in the refractive index of a crystal when exposed to an electric field[5]. Light propagating through an electro-optic medium is phase modulated by the change in refractive index, which can be converted to amplitude modulation using interferometry. Significant work has been carried out at the University of British Columbia on integrated-optic sensors. Passive immersion type devices for high-voltage measurements were proposed by Ahmed in 1981[6], integrated sensors based on Mach-Zehnder modulators were proposed by Jaeger in 1985[7,8] and most recently Jaeger's integrated-optics Pockels cell (IOPC)[9] was used to develop and implement a voltage sensor by Rahmatian *et al.*[10]

[*] sameerc@ece.ubc.ca; phone: 1 604 822-6268; fax 1 604 822-5949

Photonics North 2006, edited by Pierre Mathieu, Proc. of SPIE Vol. 6343, 634317, (2006)
0277-786X/06/$15 · doi: 10.1117/12.707707

One way of realising an entirely fiber-based sensor-head is by way of a class of fiber sensors known as evanescent wave sensors[11]. They are based on affecting the propagation of light in the fiber by modulating/changing the evanescent field that penetrates into the cladding of the fiber. With a sufficiently thin cladding, the evanescent field can extend into the medium surrounding the cladding, and to realise a sensor this surrounding medium is chosen so that it is sensitive to the measurand. The advantage of these sensors is the ability to keep the light in the fiber, i.e., removing the need to couple the light in and out.

A lot of effort has been directed towards liquid crystals which exhibit electro-optic behaviour. Room temperature liquid crystals are available and have indices of refraction close to and/or similar to those of optical fibers. In particular, chiral Smectic A (SmA*) liquid crystals are ideal as they allow for continuous modulation of their refractive indices via the electroclinic effect, allowing for their use in analog applications (unlike nematic liquid crystals, which require threshold electric fields to cause changes in their refractive indices)[12].

Sneh and Johnson have demonstrated a continuously tunable liquid crystal filter[13] using a SmA* liquid crystal as the active cavity material in a Fabry-Perot étalon. Sirleto *et al.* have demonstrated a continuously tunable filter based on a Bragg grating in a planar waveguide with a SmA* liquid crystal overlayer[14]. There has also been some effort in electric field sensors using fibers and liquid crystals. Lacquet *et al.*[15] developed an electric field probe using a polymer dispersed liquid crystal inserted between two multimode optical fibers, Anagni *et al.*[16] used a liquid crystal cell to develop an electric field presence detector and Sato *et al.*[17] demonstrated electric field measurements, covering a wide range, using a chiral liquid crystal cell placed between two optical fibers, which behaved like a polarizer. The above sensors are not in-line fiber devices and require interruption of the light in the fiber and propagation through the liquid crystal.

In this paper we present the design, investigation and fabrication of an in-line electric field sensor that uses a D-shaped optical fiber and SmA* liquid crystals. D-fibers allow easy access to the evanescent field, as the core of the fiber is typically less than 20 μm below the flat of the fiber. This cladding thickness can be reduced by etching the fiber. We have investigated the characteristics of our D-fiber with varying cladding thicknesses and external medium refractive indices. A theoretical model has been developed and verified experimentally to demonstrate the viability of our design architecture.

Including this introduction, this paper consists of five sections. In section 2 we present the theory of operation for our sensor, including the theoretical foundation and its verification experimentally. In Section 3 we discuss the various aspects of the physical design of the sensor including liquid crystals, and the particular design architecture and fabrication method used for the prototype sensor. In Section 4 we show the experimental setup and experimental results of a prototype sensor. Finally, concluding remarks are given in Section 5.

2. THEORY OF OPERATION

2.1 Theoretical foundation

Typically, in a step-index fiber with a circular cross section, the refractive index of a fiber's core, n_{co}, is greater than that of its cladding, n_{cl}, and the fiber mode effective index, n_{eff}, lies between n_{co} and n_{cl}. In the case of a D-fiber having a D-shaped cross section, the cladding between the core and fiber flat can be made to be sufficiently thin to allow the evanescent field to extend into the external medium above the fiber flat. If the fiber flat is coated with a material with refractive index n_{ext}, the mode effective index of the D-fiber/external medium structure will depend on the cladding thickness and the value of n_{ext}. When $n_{ext} \approx n_{eff}$, the fiber mode becomes leaky and power can be radiated out of the core of the fiber and the mode remains leaky for values of $n_{ext} > n_{eff}$.

Fig. 1 shows a conceptual diagram, not to scale, of our D-fiber sensor with its flat surface coated with an external medium, thick enough to act as a semi-infinite superstrate. The amount of power radiated out of the core, when the fiber mode is leaky, depends on the core dimensions, the cladding thickness, d, the length of fiber coated with the external medium, L, and the values of n_{eff} and n_{ext}. The cladding thickness is defined as the minimum distance between the fiber flat and the core edge and can be reduced from its initial value by etching, e.g., in hydrofluoric (HF) acid[18]. The fiber used in our work has an elliptical core and is polarization maintaining.

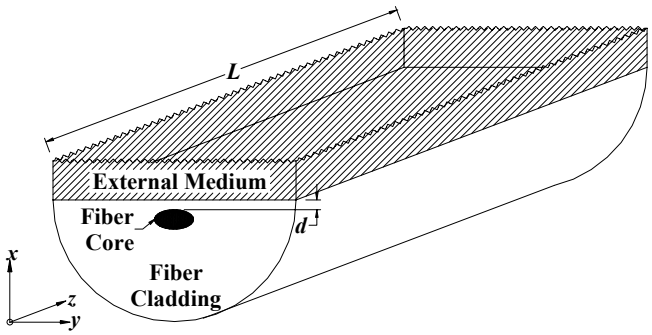

Fig. 1. Conceptual diagram of D-fiber sensor with its flat side coated with an external medium

To theoretically model the combination of the D-fiber/external medium structure, we use the method proposed by Sharma *et al.*[19] to analyze fibers with their claddings limited by a plane. The first step in the model is to replace the fiber with a three-layer equivalent planar waveguide (EPW) by matching the modal fields and propagation constants of the fiber to that of its EPW. This matching is only required for the fiber's phase constants along the direction of interaction (the *x*-direction, see Fig. 1) and the direction of propagation (the *z*-direction). Consequently, in our case, of the two core dimensions, only the semiminor axis plays a role in determining the EPW as it is the tail of the evanescent field in the *x*-direction that interacts with the external medium. This EPW is then extended to a four-layer waveguide to take into account the external medium. For the case where $n_{ext} \geq n_{eff}$, the propagation constant for the leaky TE_0 mode is given analytically by Thyagarajan *et al.*[20] and is complex, with real and imaginary parts, β_r and β_j, respectively. The power transmission, T_p, can then be written in terms of the power into, P_{in}, and the power out of, P_{out}, a section of fiber of length L, as

$$T_p = \frac{P_{out}}{P_{in}} = e^{-2\beta_j L} \tag{1}$$

Equation (1) has been used to calculate the power transmission of the TE_0 mode for a 1 cm length of our D-fiber as a function of n_{ext} for several values of d, as shown in Fig. 2. There are three distinct regions of interest with regard to the power transmission. As expected, in Region 1, where $n_{ext} < n_{eff}$, there is no loss. In Region 2, where $n_{ext} \quad n_{eff}$, the transmission decreases sharply to a minimum value and is very sensitive to changes in n_{ext}. In Region 3, where $n_{ext} > n_{eff}$, the transmission increases from the minimum value monotonically. As expected, for a particular value of n_{ext}, the transmission decreases with decreasing d, a result of the evanescent field extending further into the external medium.

It is in Regions 2 or 3 where the proposed sensor would be operated, depending on the external medium used. Region 2 is better suited due to its high sensitivity; however, one needs an external medium having $n_{ext} \quad n_{eff}$. Region 3 provides greater freedom with regard to the choice of external medium.

The imaginary part of the propagation constant for the leaky TE_0 mode, β_j, will change when an electric field, E_{app}, is applied and can be written as

$$\beta_j = \beta_{jo} + \sigma E_{app} \tag{2}$$

where β_{jo} and σ are constants based on the chosen operating point. For small changes in β_j (i.e., $\sigma E_{app} << \beta_{jo}$), Equation (1) can be linearized and rewritten as

$$T_p = e^{-2\beta_{jo}L} - 2e^{-2\beta_{jo}L}\sigma L E_{app} \tag{3}$$

The first term in the above equation is the static transmission of the sensor and the second term is the field dependent transmission.

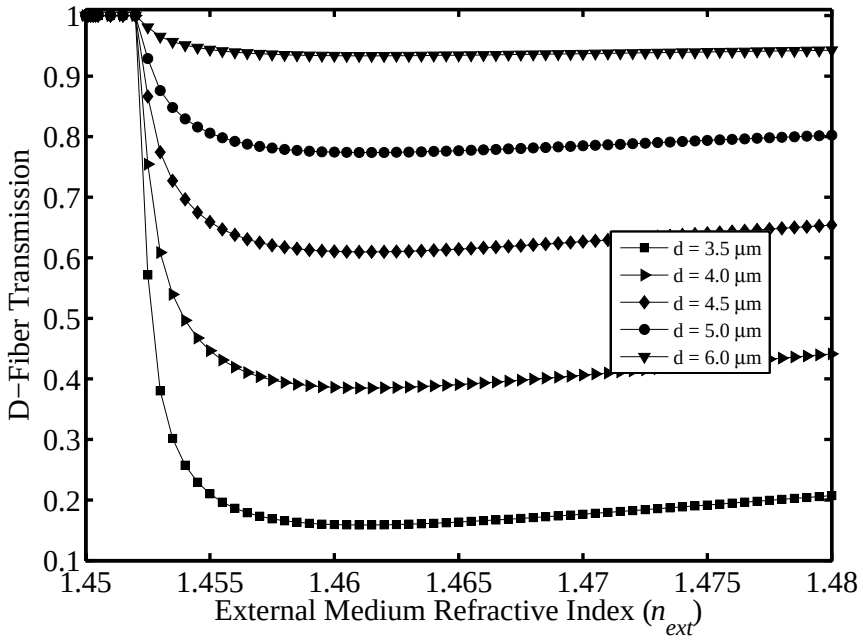

Fig. 2. Calculated transmission for the TE_0 mode versus n_{ext} for several values of d using n_{co} = 1.4756, n_{cl} = 1.441, L = 1 cm at 1550 nm.

2.2 Experimental verification

To verify the theoretical model describing the propagation characteristics of our sensor's structure, an external medium that could span all three regions was chosen. We immersed as etched section of our D-fiber in a thermo-optic oil so that changing the oil's temperature would change its refractive index[21]. The experimental setup is shown in

Fig. 3. The ends of the D-fiber were connected to standard fibers to transmit light at 1550 nm into and out of it. The D-fiber was threaded through an aluminum plate that had a trench in it to contain the oil. The plate also served as the cold plate for the thermoelectric cooler (TEC) that controlled the temperature of the oil. The polarization controller (PC) was used to launch TE_0 polarized light into the D-fiber. The output was detected using a power meter. The temperature range for our TEC was 15°C to 85°C. The index of refraction at 25°C and the thermo-optic coefficient of the oil are given by the manufacturer as 1.472 and -3.86×10^{-4}/°C, respectively, at 1550 nm. Thus, the refractive index of the oil could be changed from approximately 1.449 to 1.476, which covers the entire range in Fig. 2. Shown in Fig. 4 is the measured transmission for an etched fiber along with the best fit curve obtained using our model, which takes into account the thermo-optic effect of the silica. There is excellent agreement between measured and calculated values indicating that the model can correctly predict our structures' propagation characteristics. We have further validated our model by imaging the cross-section of the etched region using a scanning electron microscope[22].

3. PHYSICAL DESIGN

3.1 Liquid crystals

The choice for the electro-optic material to be used depends mostly on its sensitivity to electric fields, compatibility with silica, and frequency response. Liquid crystal materials are a good choice for several reasons. They are well understood, are readily available, have refractive indices close to that of silica, and can respond to frequencies from DC into the MHz range.

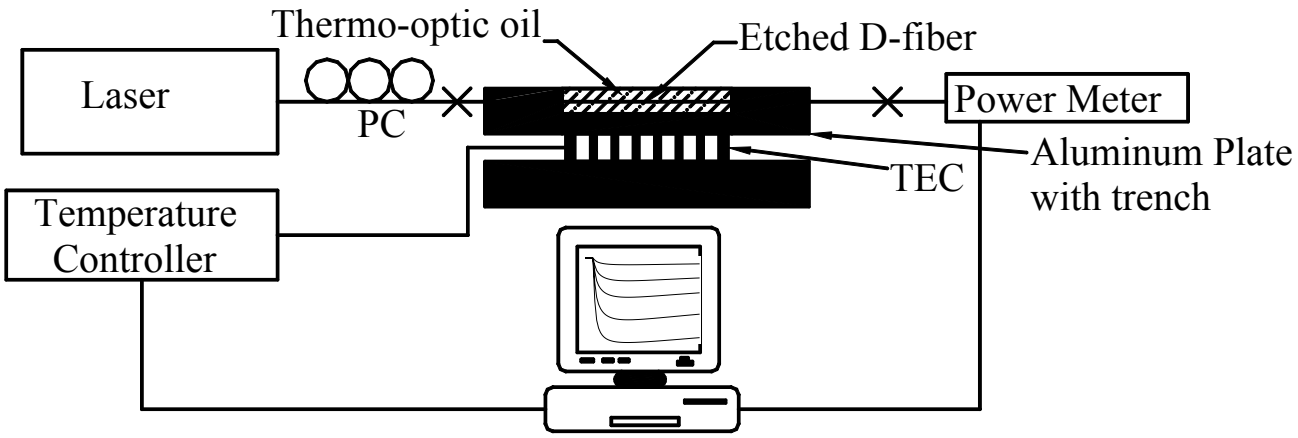

Fig. 3. Experimental setup showing etched section of fiber immersed in thermo-optic oil. TEC - Thermoelectric Cooler; × – Fiber connector; PC – Polarization Controller.

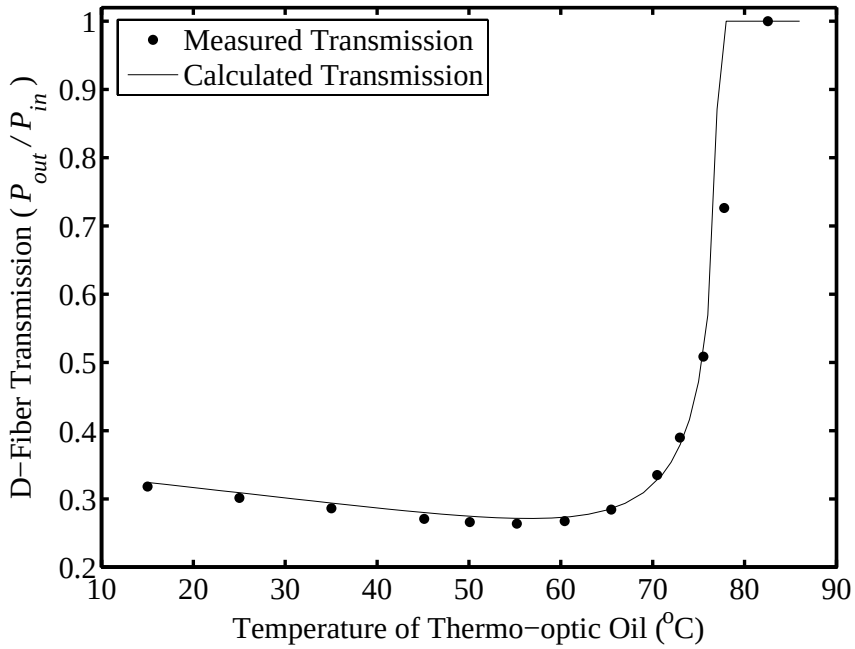

Fig. 4. Measured and calculated power transmission (using d = 3.99 μm) for a 1 cm length of etched D-fiber.

Liquid crystals are materials that show mesophases between the isotropic liquid and the crystal phases of the material and occur over well-defined temperature ranges. The material is typically made of rod like molecules that have some molecular ordering which can be affected by external electric fields. The average direction of the molecules is known as the director, $\tilde{n}$, and the optic axis is parallel to $\tilde{n}$. Liquid crystals are anisotropic materials with extraordinary refractive index, n_e, along $\tilde{n}$ and ordinary refractive index, n_o, perpendicular to $\tilde{n}$. When an electric field is applied, the director can be rotated and, thus, the refractive index seen by polarized light can be modified.

The liquid crystals (LCs) being proposed for this work are chiral (indicated by the 'asterisk' sign) smectics. In the smectic A (SmA*) phase, in particular, LCs form a layered structure with the molecules aligned parallel to each other

within each layer, so that the director is normal to the layer interfaces. The layer thickness is of the order of one molecular length. Application of an electric field perpendicular to the molecular axis causes a tilt of the director away from the layer normal by the electroclinic effect[23]. The molecular tilt results in an induced polarization along the applied electric field. The tilt angle, θ, is linear with the applied field, up to a saturation tilt, and is governed by the electroclinic coefficient, χ, and is given as

$$\theta = \chi \vec{E}_{app} \tag{4}$$

3.2 Design Architecture

The possible design architectures are dictated by how the LCs are aligned along the surface of the fiber flat. There are two ways in which LCs align themselves to surfaces; homogeneous and homeotropic. Homogeneous alignment is when the rod like molecules are aligned parallel to the surface and homeotropic alignment is when they are perpendicular to the surface. Homogeneous alignment can be achieved simply by coating the surface with an appropriate solution, and rubbing it with a soft tissue or a brush – the rod like molecules align themselves along the direction of rubbing. Homeotropic alignment can be achieved using appropriate surfactants on the surface.

Fig. 5 shows the design architecture used for our sensors. Top and cross sectional views of the D-fiber are shown with the directions of $\tilde{E}_{app}$, n_o, n_e, and $\tilde{n}$ indicated. The liquid crystals are homogeneously aligned at an angle θ_o with respect to the fiber axis. An electric field applied normal to the D-fiber flat rotates the LC molecules by a small angle $\delta\theta$. Consequently, the TM mode of the fiber always sees n_o and its propagation constant is not affected by the applied field. Hence, in the sensor reported on here, we only excited the TE mode. The TE mode sees $n_\theta(\theta_o \pm \delta\theta)$ depending on the direction of $\tilde{E}_{app,}$ where

$$n_\theta(\theta) = \frac{n_e n_o}{\sqrt{n_o^2 \sin^2\theta + n_e^2 \cos^2\theta}} \tag{5}$$

and θ is the angle between the polarization direction of the light and the optic axis[24]. n_θ is set to an operating point by fixing θ_o so that small changes of $\delta\theta$ by the electroclinic effect results in changes in n_θ, which results in changes in the TE mode's power. The LC that was readily available to us had both n_o and $n_e > n_{eff}$ so that the sensor operated in Region 3.

We would like to point out that the fact that the two modes of the fiber see different refractive indices opens up the possibility of designing an interferometric sensor in which both the modes are excited. An LC would have to be engineered to have n_o and $n_\theta < n_{eff}$ so that both modes are guided and only the TE mode propagation constant would be affected by the electric field. In such a sensor, interference of the two modes at the output of the sensor would be used to detect the electric field, similar to what is done in crystal-based electric field sensors.

3.3 Fabrication technique

To fabricate a sensor a film of properly aligned liquid crystals must be placed over the flat of the D-fiber. This can be achieved using several techniques. Here we describe the technique used to fabricate our prototype sensor. Fig. 6 shows the cross section of our fabricated sensor. In order to apply an electric field, the sensor was sandwiched between two electrodes; an aluminium base and an indium tin oxide (ITO) coating on the top cover. The D-fiber was etched for ~150 min so that the cladding thickness was reduced to ~ 5 μm, which provides an appreciable loss as seen in Fig. 2. The etched section of the D-fiber was bonded with its flat side facing up into a groove machined into a plastic cover slip. W415, the liquid crystal material used, has a SmA* phase between 34.3°C and 24.1°C and an electroclinic coefficient of approximately 1.3 deg/(V/μm) at 30°C[25]. For correct planar alignment of the liquid crystal molecules, the LC requires the coating of both surfaces with a nylon solution and the rubbing of one or both of the surfaces with a brush to force the alignment of the crystals along the rubbing direction. The nylon solution was spun onto the fiber flat and onto the ITO coated side of the top cover. The fiber flat was then rubbed with a brush along the fiber axis. The LC, in its isotropic

phase (T = 50°C), was inserted into the cavity created around the fiber through capillary action and cooled to its SmA* phase (T = 30°C) at a rate of -0.1°C/min.

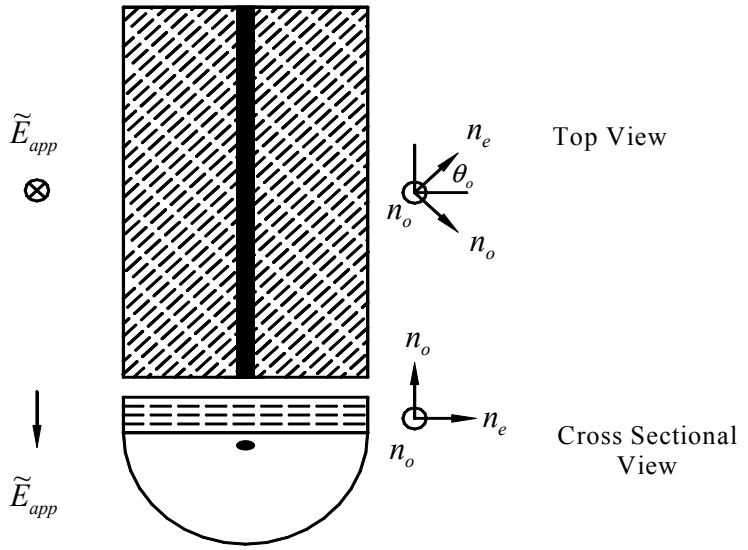

Fig. 5. Top and Cross sectional view of sensor with liquid crystal aligned at θ_o to the fiber axis. Shown for each view are the directions n_o and n_e, the LC director, $\tilde{n}$, and the direction of $\tilde{E}_{app}$

4. EXPERIMENTAL SETUP AND RESULTS

The experimental setup used to verify the prototype is shown in Fig. 7. A lock-in amplifier (LIA) was used to apply and detect the electric field. Its output was amplified using a high voltage amplifier capable of applying a maximum of $200V_{pk}$. The frequency of primary interest for high voltage applications is either 50 or 60 Hz, and here we used a 50 Hz sinusoid.

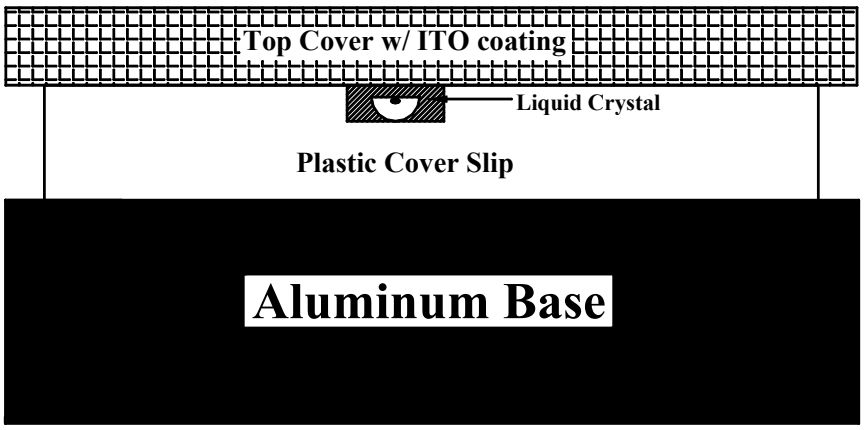

Fig. 6. Cross section of fabricated sensor

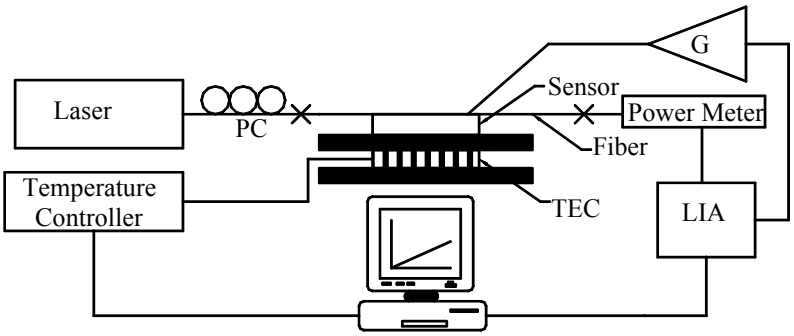

Fig. 7. Experimental setup. TEC - Thermoelectric Cooler; × – Fiber connector; PC – Polarization Controller; LIA – Lock-in Amplifier; G – High Voltage Amplifier.

The temperature of the LC was set to either 29 or 30°C so that the LC was in its SmA* phase. The voltage applied to the sensor was ramped up and down in 25 V steps between zero and its peak value of 200 V. Many such ramps were conducted in succession. For each voltage level within a ramp, the LIA signal was sampled every second for 60 seconds and the mean and standard deviation of the 60 samples was calculated. Based on the geometry of the sensor and the field reduction factor due to the induced depolarization field[26], the peak electric field in the liquid crystal layer was estimated to be ~ 0.45 V/μm.

Fig. 8 shows the prototype sensor's response at the two different temperatures. As expected, the sensor's response to a ramped AC applied voltage is linear; however, we found that the slope of the response changed over time. Also shown in the figure is this evolution of slope of the sensor's linear response. To demonstrate the linearity of the sensor, Fig. 9 shows the curve in Fig. 8 with the largest slope, along with error bars and a linear fit. The error bars are the standard deviation of the mean of the samples taken at each voltage level.

Obviously, this time dependent change in the signal is unwanted and unexpected. We feel there are several possible reasons for this. As mentioned earlier, the alignment of the LC molecules is very important and one possible reason for this time dependent change is that the surface of the fiber flat was not optimally treated, causing imperfect alignment of the molecules. The slope of the sensor's response starts off small and increases to a peak. It is possible that the application of the electric field over time forces or aids some improperly aligned molecules to align themselves with any properly aligned neighbouring molecules. Another possible reason could be the LC film thickness. In the majority of liquid crystal applications, such as in display applications, the liquid crystals are confined between two glass slides with a spacing on the order of 1-5 μm. In our case, the molecules are confined to a spacing of > 20 μm, which may have also affected the alignment of the molecules. Further process development is necessary to optimally align the liquid crystals on the fiber flat.

5. SUMMARY

We have proposed a design for an in-line electric field sensor using evanescent fields in D-fibers and chiral liquid crystals. Fabrication and testing of our prototype show proof of principle. The sensor responds linearly to an applied electric field and has a peak sensitivity of 0.2 mV/(V/μm), but we found that the sensitivity changed over time. It is likely that improvements would be possible using a liquid crystal that could be specifically tailored for this application.

ACKNOWLEDGMENTS

We would like to thank David Walba for supplying the liquid crystal material used in these studies. This research has been supported in part by NSERC and the NSERC eMPOWR program administered through Canadian Institute for Photonic Innovations (CIPI).

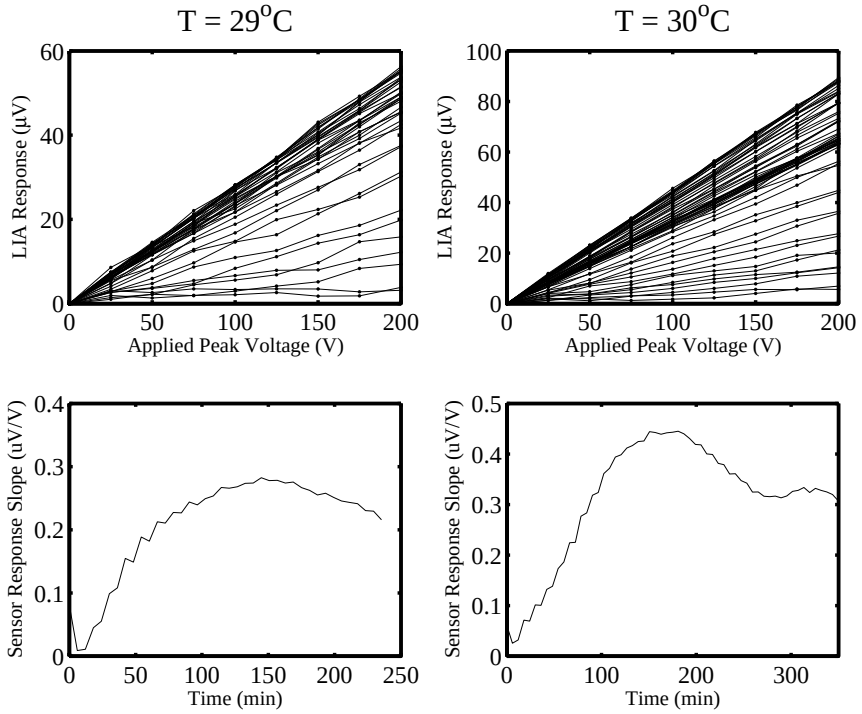

Fig. 8. Prototype sensor response to voltage ramps for liquid crystal temperatures of 29 and 30°C along with slope of sensor's linear response.

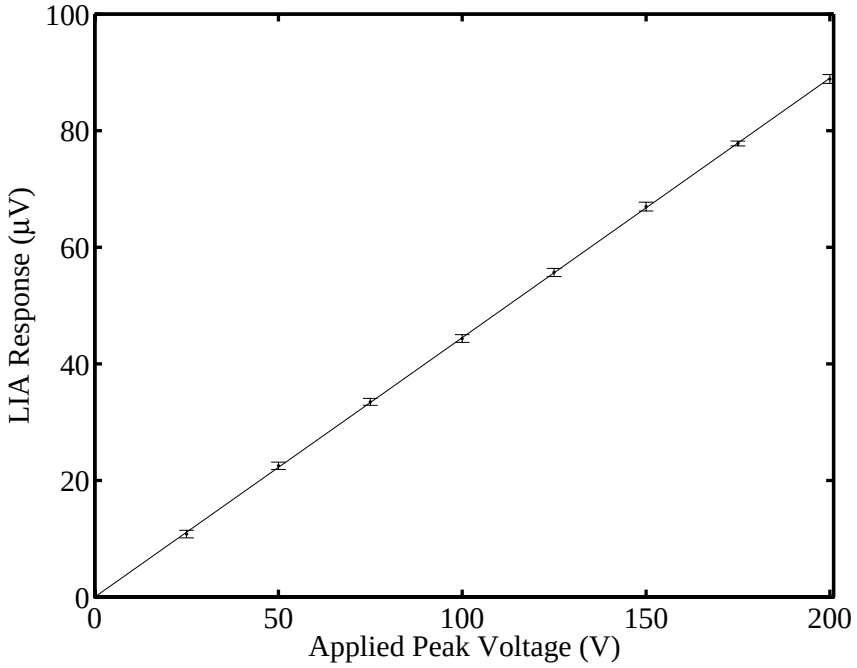

Fig. 9. Largest slope sensor response along with error bars and linear fit

REFERENCES

1. A.J. Rogers, "Optical technique for the measurement of current at high voltage," in *Proc.of IEE*, vol. 120, no. 2, pp. 261-267, 1973.
2. G.A. Massey, D.C. Erickson, and R.A. Kaldec, "Electromagnetic field components: Their measurement using linear electro-optic and magnetooptic effects," *Applied Optics*, vol. 14, no. 11, pp. 2712-2719, 1975.
3. A.J. Rogers, "method for simultaneous measurement of current and voltage on a high-voltage lines using optical techniques," in *Proc.of IEE*, vol. 123, no. 10, pp. 957-960, 1976.
4. R.E. Hebner, R.A. Malewski, E.C. Cassidy, "Optical methods of electrical measurements at high voltage levels," in *Proc. of IEEE*, vol. 65, no. 11, pp. 1524-1548, 1977.
5. J. A. Valdmanis, "*Electro-optic measurement techniques for picosecond materials, devices, and integrated circuits*," in Measurement of High-Speed Signals in Solid State Devices, edited by R. B. Marcus, Academic Press, San Diego, pp. 136-217, 1990.
6. M.J. Ahmed, "*Integrated optical devices in lithium niobate*," Ph.D. dissertation, University of British Columbia, Vancouver, B.C., Canada, 1981.
7. N.A.F. Jaeger, "*Integrated optical devices in lithium niobate*," M.A.Sc thesis, University of British Columbia, Vancouver, B.C., Canada, 1985.
8. N.A.F. Jaeger, L. Young, "High-voltage sensor employing an integrated optics Mach-Zehnder interferometer in conjunction with a capacitive divider," *Journal of Lightwave Technology*, vol. 7, no. 2, pp. 229-235, 1989.
9. N.A.F. Jaeger, "Integrated Optics Pockels Cell Voltage Sensor," U.S. Patent #5,029,273, July 2, 1991.
10. F. Rahmatian, "*Integrated optics Pockels cell high voltage sensor*," M.A.Sc. thesis, University of British Columbia, Vancouver, B.C., Canada, 1993.
11 C.M. Davis, "Fiberoptic sensors: an overview," in *Proc. of SPIE*, 1983, vol. 412, pp. 2-8.
12. G. Andersson *et al.*, ''Device physics of the soft mode electro-optic effect,'' *Journal of Applied Physics*, vol. 66, no. 10, pp. 4983-95, 1989.
13. Sneh, A., Johnson, K.M., "High-speed continuously tunable liquid crystal filter for WDM networks," *Journal of Lightwave Technology,* vol. 14**,** no. 6, pp. 1067-1080, 1996.
14. Luigi Sirleto *et al.*, "Electro-optical switch and continuously tunable filter based on a Bragg grating in a planar waveguide with a liquid crystal overlayer," *Optical Engineering,* vol. 4, no.11, pp. 2890–2898, 2002.
15. Lacquet, B.M., Swart, P.L., Spammer, S.J., "Polymer dispersed liquid crystal fiber-optic electric field probe," *IEEE Transactions on Instrumentation and Measurement*, vol. 46, no. 1, pp. 31-51, 997.
16. Anagni, F., Bartoletti, C., Marchetti, U., Podesta, L., Sacerdoti, G., "Optical sensors for electric substations: a voltage presence detector using a liquid crystal cell," *IEEE Transactions on Instrumentation and Measurement*, vol. 43, no. 3, pp. 475-80, 1994.
17. S. Sato and T. Hara, "Applications of a ferroelectric liquid-crystal cell to an electric field sensor," *Jpn. J. Appl. Phys.,* vol. 32, pp. 3664–3665, 1993.
18. Selfridge, R.H., Pugmire, G.T., Curtis, M., "In-situ monitoring of D-type fiber etching," in *Proc. of SPIE,* 1989, vol. 1168, pp. 314-322.
19. A. Sharma, J. Kompella, P.K. Mishra, "Analysis of fiber directional couplers and coupler half-blocks using a new simple model for single-mode fibers," *Journal of Lightwave Technology*, vol. 8, no. 2, pp. 143-151, 1990.
20. K. Thyagarajan, S. Diggavi, A.K. Ghatak, "Analytical investigations of leaky and absorbing planar structures," *Optical and Quantum Electronics*, vol. 19, no. 2, pp. 131-137, 1987.
21. S.M. Chandani and N.A.F. Jaeger, "Fiber-optic temperature sensor using evanescent fields in D fibers", *IEEE Photonics Technology Letters*, vol. 17, no. 12, pp. 2706-8, 2005.
22. S.M. Chandani, A. Kulpa, N.A.F. Jaeger, "Non-destructive Determination of Cladding Thickness in D-fibers," *IEEE Photonics Technology Letters,* vol. 18, no. 9, pp. 1082-84, 2006.
23. S. Garoff and R. B. Meyer, 'Electroclinic Effect at the A-C Phase Change in a Chiral Smectic Liquid Crystal', *Phys. Rev. Lett.*, vol. 38, no. 15, pp. 848, 1977.
24. C. C. Davis, *Lasers and Electro-Optics: Fundamentals and Engineering*, Cambridge University Press, Cambridge, 1996, pp. 448.
25. R-F. Shao, J.E. Maclennan, N.A. Clark, D.J. Dyer, D.M. Walba, "Giant surface electroclinic effect in a chiral smectic A liquid crystal," *Liquid Crystals*, vol. 28, no. 1, pp. 117-23, 2001.
26. C. Kittel, Introduction to solid state physics, Wiley, New York, 1956, pp. 157.